Magnetic Field and Pressure Phase Diagrams of Uranium Heavy-Fermion Compound U_2Zn_{17}*

Naoyuki TATEIWA[1]†, Shugo IKEDA[1,2], Yoshinori HAGA[1], Tatsuma D. MATSUDA[1], Etsuji YAMAMOTO[1], Kiyohiro SUGIYAMA[3], Masayuki HAGIWARA[4], Koichi KINDO[5], and Yoshichika ŌNUKI[1,3]

[1]*Advanced Science Research Center, Japan Atomic Energy Agency, Tokai, Ibaraki 319-1195*
[2]*Graduate School of Material Science, University of Hyogo, Kamigori, Hyogo 678-1297*
[3]*Graduate School of Science, Osaka University, Toyonaka, Osaka 560-0043*
[4]*KYOKUGEN, Osaka University, Toyonaka, Osaka 560-8531*
[5]*Institute for Solid State Physics, University of Tokyo, Kashiwa, Chiba 277-8581*

We have performed magnetization measurements at high magnetic fields of up to 53 T on single crystals of a uranium heavy-fermion compound U_2Zn_{17} grown by the Bridgman method. In the antiferromagnetic state below the Néel temperature $T_N = 9.7$ K, a metamagnetic transition is found at $H_c \simeq 32$ T for the field along the $[11\bar{2}0]$ direction (a-axis). The magnetic phase diagram for the field along the $[11\bar{2}0]$ direction is given. The magnetization curve shows a nonlinear increase at $H_m \simeq 35$ T in the paramagnetic state above T_N up to a characteristic temperature $T_{\chi max}$ where the magnetic susceptibility or electrical resistivity shows a maximum value. This metamagnetic behavior of the magnetization at H_m is discussed in comparison with the metamagnetic magnetism of the heavy-fermion superconductors UPt_3, URu_2Si_2, and UPd_2Al_3. We have also carried out high-pressure resistivity measurement on U_2Zn_{17} using a diamond anvil cell up to 8.7 GPa. Noble gas argon was used as a pressure-transmitting medium to ensure a good hydrostatic environment. The Néel temperature T_N is almost pressure-independent up to 4.7 GPa and starts to increase in the higher-pressure region. The pressure dependences of the coefficient of the T^2 term in the electrical resistivity A, the antiferromagnetic gap Δ, and the characteristic temperature $T_{\rho max}$ are discussed. It is found that the effect of pressure on the electronic states in U_2Zn_{17} is weak compared with those in the other heavy fermion compounds.

KEYWORDS: U_2Zn_{17}, magnetic phase diagram, pressure phase diagram

1. Introduction

Uranium intermetallic compounds exhibit unique electronic states such as magnetic orderings, heavy fermions, and anisotropic superconductivity.[1–3] These properties are basically derived from the competition between the Ruderman-Kittel-Kasuya-Yosida (RKKY) interaction and the hybridization (Kondo) effect. The former interaction enhances the long-range magnetic order, where $5f$ electrons with magnetic moments are treated as localized electrons and the indirect $5f$-$5f$ interaction is mediated by the spin polarization of the conduction electrons. On the other hand, the latter effect quenches the magnetic moments of the localized $5f$ electrons by the spin polarization of the conduction electrons, leading to an extremely large density of states, called heavy fermions.

The application of pressure is a useful experimental method for controlling the magnetic RKKY interaction and hydridization effect. As pressure is applied to some compounds with magnetic orderings, the magnetic ordering temperature T_{mag} decreases and becomes zero at a critical pressure P_c: $T_{mag} \to 0$ at $P \to P_c$, where the pressure-induced superconductivity or non-Fermi liquid behavior appears. The pressure dependence of the magnetic ordering temperature T_{mag} in cerium compounds is basically explained by the Doniach model, in which the magnetic ordering temperature T_{mag} varies as a function of $|J_{cf}|D(\varepsilon_F)$,[4] where $|J_{cf}|$ is a magnitude of the magnetic exchange interaction between the localized moment and the conduction electron spin, and $D(\varepsilon_F)$ is the electronic density of states at the Fermi energy ε_F. The pressure-induced superconductivity was discovered around P_c in some cerium antiferromagnetic compounds such as $CeCu_2Si_2$, $CeRh_2Si_2$, $CePd_2Si_2$, $CeIn_3$, and $CeRhIn_5$.[5–8] On the other hand, pressure experiments on uranium compounds are small in number, and moreover, the pressure effect in uranium compounds seems to be small compared with that in cerium compounds of which the critical pressures P_c are usually below 10 GPa. The pressure-induced superconductivity was only observed below P_c of the ferromagnetic state in UGe_2 and UIr.[9–12]

In this study, we focus on the uranium heavy-fermion antiferromagnet U_2Zn_{17} and studied its electrical and magnetic properties at a high magnetic field and a high pressure. U_2Zn_{17} crystalizes in the rhombohedral Th_2Zn_{17}-type structure (space group $R\bar{3}m$).[13,14] At ambient pressure, U_2Zn_{17} shows antiferromagnetic ordering at a Néel temperature $T_N = 9.7$ K with an ordered magnetic moment $\mu_{ord} = 0.8\ \mu_B$/U.[15,16] The ordered moment is substantially below the paramagnetic moment of 3.15 μ_B/U deduced from the high-temperature magnetic susceptibility measurement on a single crystal sample.[17]

*J. Phys. Soc. Jpn. **80** 014706 (2011).
†E-mail address: tateiwa.naoyuki@jaea.go.jp

The specific heat coefficient C/T shows a large value of about 500 mJ/K^2·molU above T_N but is reduced to about $\gamma = 200$ mJ/K^2·mol at $T \ll T_N$.[13] These results reveal the heavy-fermion nature of an itinerant-5f electronic state in U_2Zn_{17}. A previous high-pressure experiment on U_2Zn_{17} showed that the antiferromagnetic ordering temperature T_N increases slightly with increasing pressure from $T_N = 9.70$ K at 1 bar to 9.85 K at 1.72 GPa.[18,19] In this study, we have measured the magnetization under high magnetic field, as well as performed the resistivity measurement under high pressures of up to 9 GPa using a diamond anvil cell.

2. Experimental Methods

A single-crystal sample of U_2Zn_{17} was obtained by the Bridgman method with a W crucible sealed with argon gas. The crucible was kept at 950-1050 °C for 12 h and then cooled down slowly at a constant rate. The crystal structure was investigated by single-crystal X-ray diffraction techniques using an imaging plate (IP) area detector (Rigaku Corporation) with Mo $K\alpha$ radiation at room temperature.

The electrical resistivity at both ambient and high pressures was measured by the four-probe DC method in the temperature range from 2 to 300 K. The magnetic susceptibility and magnetization were measured using a commercial superconducting quantum interference device (SQUID) magnetometer in the temperature range from 2 to 300 K. The high-field magnetization was measured by the standard pick-up coil method at the High-Magnetic-Field Laboratory, KYOKUGEN, Osaka University, using a long-pulse magnet with a pulse duration of 20 ms.

For the high-pressure study, a small sample was cut and polished to 180×50×20 μm^3. Four gold-wires 10 μm in diameter were bonded to the sample using silver paste. We used a diamond anvil cell of the Dunstan and Spain-type.[20,21] The sample and small ruby chips were placed in a sample hole 400 μm in diameter of a stainless-steel gasket in DAC. The culet-size of the diamonds is 800 μm. The electrodes are insulated from the metal gasket using a mixture of Al_2O_3 powder and stycast 1266.[20–23] For a pressure-transmitting medium, we used the noble gas argon (Ar), which is known to provide a good hydrostatic condition up to 10 GPa at room temperature.[24,25] We confirmed that argon is also appropriate as the pressure-transmitting medium in the cryogenic experiment under high pressure.[26] Argon can be liquefied at 87 K. It was loaded into the sample chamber of DAC using a purpose-built cryogenic device. The pressure was determined by the ruby fluorescence method at room temperature and 4.2 K.[27–29] We used the hydrostatic ruby pressure scale obtained by Zha *et al.*[30] Some ruby chips with a diameter less than 5 μm are placed in the sample chamber. Note that the pressure does not change significantly during the cooling process for the present DAC. The difference between the pressure at 4.2 and 300 K is less than 5%. This is different from the other types of diamond anvil cells where the pressure at low temperatures is usually about 1 GPa higher or lower than that at room temperature. In the following, the pressure determined at 4.2 K will be shown.

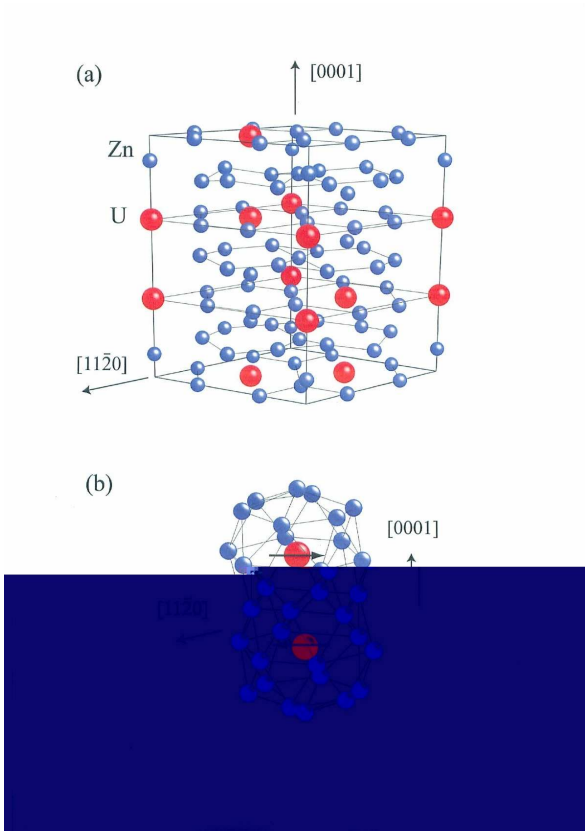

Fig. 1. (Color online) Crystal structure in U_2Zn_{17}.

3. Results and Discussion

3.1 *Crystal structure of U_2Zn_{17}*

Figure 1(a) and 1(b) show the crystal structure of U_2Zn_{17}. Crystallographic parameters for U_2Zn_{17} at room temperature is shown in Table I. The lattice parameters are a =8.9830(4)Å and c = 13.1800(9) Å at room temperature. The crystallographic parameters are consistent with the previous study within experimental error.[31] It is noted that the atomic coordinates in Table I are standardized using *STRUCTURE TIDY*.[32] The unit cell shown in Fig. 1 (a) containing 6 formula units (114 atoms) appears complicated. To illustrate the local environment around the uranium site, we picked up neighboring Zn atoms, as shown in Fig. 1(b). The uranium site has 19 Zn neighbors, forming a nearly spherical cage, with an open space toward the other uranium site connected to the next Zn cage. The center of mass of the unit consisting of 2 U and 32 Zn atoms shown in Fig. 1(b) is located at (0,0,1/2) and equivalent positions. The magnetic moments of the U ions in the cage, lying in the (0001) plane, are antiferromagnetically coupled in the ordered state below T_N.[15,16] The direction of the moment in the basal plane is not determined.

Table I. Crystallographic parameters for U_2Zn_{17} at room temperature in the hexagonal setting (space group $R\bar{3}m$) with lattice parameters a =8.9830(4)Å and c = 13.1800(9) Å. The conventional unweighted and weighted agreement factors of R_1 and wR_2 are 7.9 and 19%, respectively.

Atom	Site	x	y	z	B_{eq} (Å^2)
Zn(1)	18h	0.4956(3)	0.50438(16)	0.1526(2)	0.76(6)
Zn(2)	18f	0.2965(3)	0	0	0.86(6)
Zn(3)	9d	1/2	0	1/2	0.70(7)
Zn(4)	6c	0	0	0.0999(4)	0.80(8)
U	6c	0	0	0.33611(10)	0.51(5)

3.2 Resistivity and magnetic susceptibility at 1 bar

Figure 2 shows the logarithmic-scale of the temperature dependences of the electrical resistivity ρ for the currents along the $J \parallel [11\bar{2}0]$ (a-axis) and [0001] (c-axis) directions. The values of the residual resistivity ratio (RRR $= \rho_{RT}/\rho_0$) are 75 for $J \parallel [11\bar{2}0]$ and 81 for $J \parallel$ [0001], where ρ_{RT} and ρ_0 are the resistivity at room temperature and the residual resistivity, respectively, indicating a comparably high quality of the present samples. The resistivity ρ increases with decreasing temperature with a broad maximum at $T_{\rho max}$ = 18.7 and 23.5 K for $J \parallel [11\bar{2}0]$ and [0001], respectively. The resistivity shows a sharp kink at the Néel temperature T_N = 9.65 K and decreases steeply with decreasing temperature. We define T_N as the peak position in the temperature dependence of $d^2\rho/dT^2$. The overall feature of the temperature dependence of the resistivity is roughly consistent with that reported in a previous study using a polycrystal sample.[13] Thus far, the temperature dependence of the resistivity using a single crystal sample was reported only for $J \parallel$ [0001].[33] The resistivity ρ for $J \parallel [11\bar{2}0]$ is found to be approximately half as small as that for $J \parallel$ [0001] above T_N.

Figure 3(a) shows the logarithmic-scale of the temperature dependences of the magnetic susceptibility χ for the magnetic fields along the $[11\bar{2}0]$, $[10\bar{1}0]$, and [0001] directions. The magnetic susceptibilities χ for $H \parallel [11\bar{2}0]$ and $[10\bar{1}0]$ have broad maxima at $T_{\chi max} \simeq$ 17 K, which is close to $T_{\rho max}$ at which the resistivity shows a maximum. $T_{\chi max}$ or $T_{\rho max}$ corresponds to the characteristic temperature T_0 of the electronic state in U_2Zn_{17}. The susceptibility χ shows a sharp kink at the antiferromagnetic transition temperature T_N = 9.8 K and decreases steeply below T_N.

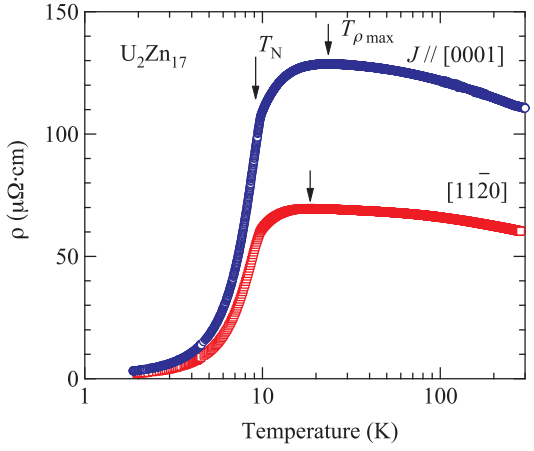

Fig. 2. (Color online) Temperature dependences of the electrical resistivity at 1 bar for currents along $J \parallel [11\bar{2}0]$ and [0001] directions in U_2Zn_{17}.

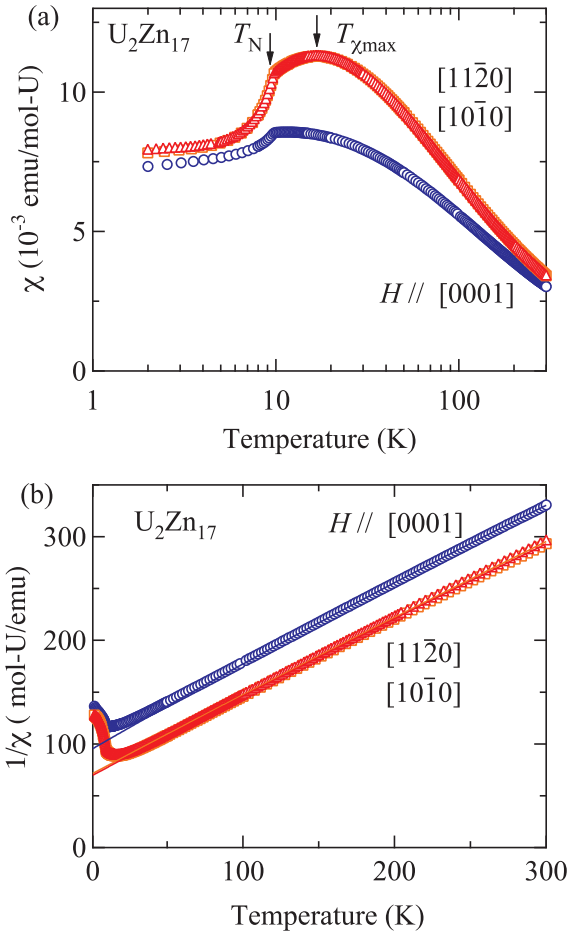

Fig. 3. (Color online)Temperature dependences of (a) the magnetic susceptibility χ and (b) the inverse susceptibility $1/\chi$ for the magnetic fields along $[11\bar{2}0]$, $[10\bar{1}0]$, and [0001] directions in U_2Zn_{17}.

The inverse magnetic susceptibility $1/\chi$ follows the Curie-Weiss law above 40 K for $H \parallel [11\bar{2}0]$ and $[10\bar{1}0]$, and above 100 K for $H \parallel$ [0001], as shown in Fig. 3(b). The effective paramagnetic moments μ_{eff} and the Curie-Weiss temperatures Θ are = 3.19 μ_B/U and - 91 K for $H \parallel [11\bar{2}0]$, 3.15 μ_B/U and -87 K for $H \parallel [10\bar{1}0]$, and 2.99 μ_B/U and Θ = -109 K for $H \parallel$ [0001], respectively. These values of μ_{eff} for $H \parallel [11\bar{2}0]$ and $[10\bar{1}0]$ are roughly similar to the values for a free U ion value of 3.6 μ_B/U in the $5f^2$ and $5f^3$ configurations.

The anisotropy of χ for three axes becomes smaller with decreasing temperature in the antiferromagnetic ordered state below T_N. In particular, there is no significant

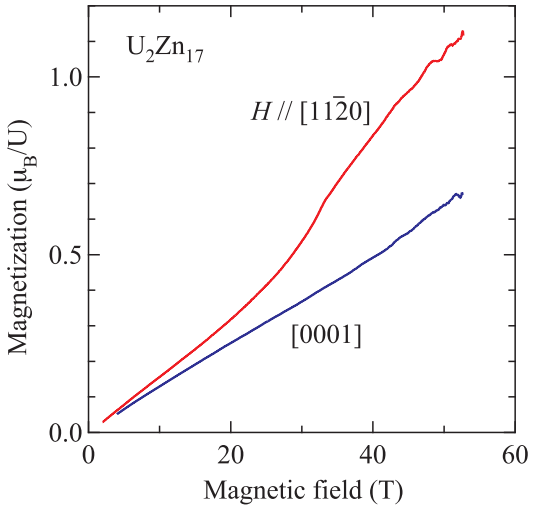

Fig. 4. (Color online) Magnetization curves in the magnetic field along [11$\bar{2}$0] and [10$\bar{1}$0] directions at 1.3 K in U_2Zn_{17}.

difference between the temperature dependences of χ for $H \parallel [11\bar{2}0]$ and $[10\bar{1}0]$ perpendicular to the [0001] direction. A previous work has shown the magnetic susceptibilities for the fields parallel and perpendicular to the [0001] direction.[17] The result is basically consistent with the result of the present work. In the present study, it was clarified that there is no anisotropy of χ inside the (0001) plane even below T_N. It is noted that the value of the critical exponent of the magnetic Bragg intensity β (= 0.36 ± 0.02) in the neutron scattering experiment for U_2Zn_{17} is between those expected for three-dimensional Heisenberg (β = 0.367) and XY (β = 0.345) magnets.[16,34] The anisotropy of the antiferromagnetic state is weak in U_2Zn_{17}.

3.3 High-magnetic-field experiment

Figure 4 shows the magnetization curves for the field along the [11$\bar{2}$0] and [10$\bar{1}$0] directions at 1.3 K. There is no strong anisotropy in the magnetization processes at a low magnetic field. The magnetization for $H \parallel [11\bar{2}0]$ increases approximately linearly with increasing magnetic field and shows a metamagnetic transition at H_c = 33 T. With further increasing field, the magnetization increases monotonically and amounts to 1.1 μ_B/U at 50 T. The present value is larger than the antiferromagnetic ordered moment (0.8 μ_B), indicating the itinerant band magnetism of 5f electrons in U_2Zn_{17}. The magnetization for $H \parallel$ [0001] increases linearly as a function of magnetic field and starts to deviate upward from about 42 T. This result suggests that the metamagnetic transition also exists for $H \parallel$ [0001] at a magnetic field higher than 52 T, the highest magnetic field in the present study.

Figure 5 (a) shows the magnetization curves in the magnetic field along the [11$\bar{2}$0] direction at various temperatures. The corresponding field derivatives of the magnetization curve, dM/dH, are shown in Fig. 5 (b). The metamagnetic transition at H_c becomes broad with increasing temperature up to 9.2 K, just below T_N = 9.65

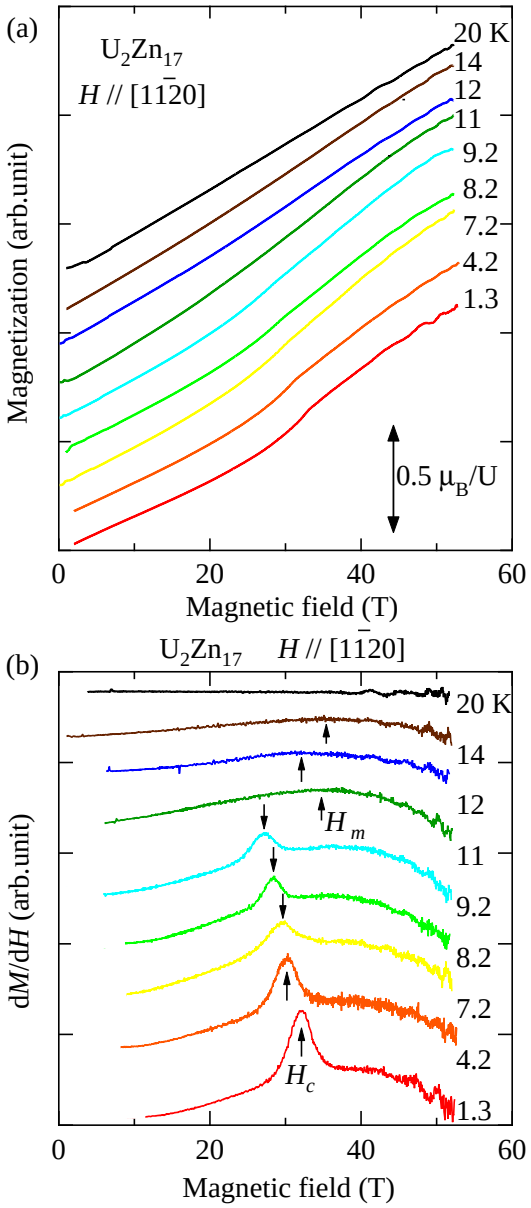

Fig. 5. (Color online) (a) Magnetization curves at various temperatures and (b) differential magnetization curves for the field along the [11$\bar{2}$0] direction in U_2Zn_{17}.

K. At 11, 12, and 14 K, the slope of the magnetization curves shows another metamagnetic behavior at H_m. In fact, there appear broad peaks at H_m in the dM/dH curves at these temperatures, as shown in Fig. 5 (b). At 20 K, the magnetization increases linearly.

Figure 6 shows the magnetic phase diagram for $H \parallel$ [11$\bar{2}$0]. The data obtained from the high-field magnetization measurement are shown by open circles and diamonds. The field dependences of T_N and $T_{\chi max}$, determined by the SQUID magnetization measurement, are shown by open squares and triangles, respectively. The metamagnetic transition field H_c in the antiferromagnetic order state decreases from 32.5 T at 1.3 K to 27.8 T at 9.2 K. A curve connecting the H_c data seems to

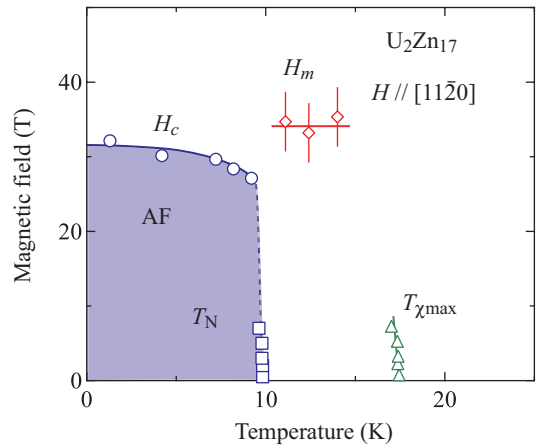

Fig. 6. (Color online) Magnetic phase diagram of U_2Zn_{17} for the field along the [11$\bar{2}$0] direction. Solid and dotted lines are a guide to the eyes.

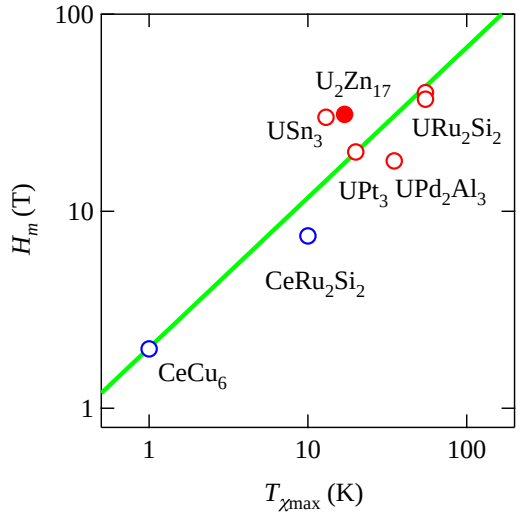

Fig. 7. (Color online) Metamagnetic anomaly fields H_m of several heavy-fermion compounds, shown in logarithmic scale. A closed circle corresponds to that in the case of U_2Zn_{17}.

reach the phase boundary of T_N below 7 T. It seems that the metamagnetic behavior at H_m in the paramagnetic state appears in the temperature region between T_N and $T_{\chi max}$.

We suggest that the metamagnetic behavior at H_m in the paramagnetic state of U_2Zn_{17} is similar to those observed for heavy-fermion compounds such as UPt_3, URu_2Si_2, and UPd_2Al_3 below $T_{\chi max}$, where the magnetic susceptibility shows a maximum.[35–37] It is basically supposed that the behavior is associated with the change of the hybridization effect between conduction electrons with a wide energy band and almost localized f-electrons.[1] Almost localized f-electrons become itinerant with decreasing temperature through the many-body effect. The crossover from localized to itinerant occurs at a characteristic temperature T_0, corresponding to $T_{\chi max}$ or $T_{\rho max}$, where the magnetic susceptibility or the electrical resistivity has a maximum. The metamagnetic behavior appears at H_m, where the relation of $k_B T_{\chi max} \simeq \mu_B H_c$ is realized by applying magnetic field, as shown in Fig. 7. The relation of $T_{\chi max} = 17$ K and $H_m = 32$ T in U_2Zn_{17} is shown in the Fig. 7 by a closed circle, approximately consistent with this relation.

Various microscopic theoretical studies have been performed on the metamagnetic behavior of the magnetization in heavy-fermion compounds. Miyake and Kuramoto have calculated the magnetization process using a semi-phenomenological model called the duality model of heavy fermions on the periodic Anderson lattice model.[38,39] In the model, the metamagnetic behavior takes place when the second derivative of the density of states is positive and the coupling between itinerant and localized parts of f electrons is large. From a different point of view, it was proposed that the anisotropy of the hybridization matrix element yields the characteristic shape of the density of states that plays a major role in the metamagnetism.[40,41] Ohkawa and coworkers clarified the spin-lattice effect cooperating with the ferromagnetic exchange interaction causes the metamagnetic behaviors.[42–44] Although a final consensus has not been established yet, the metamagnetic behavior in the heavy-fermion system is one of the important issues in f-electron magnetism. We hope that the present observation in U_2Zn_{17} stimulates future studies on the issue.

3.4 High-pressure experiment

Figure 8 (a) shows the logarithmic temperature dependence of the electrical resistivity ρ in the current parallel to the [11$\bar{2}$0] direction under high pressures. The resistivity at room temperature increases slightly with increasing pressure. The characteristic temperature $T_{\rho max}$, where the resistivity shows a maximum, is shifted to the higher temperature side with increasing pressure. $T_{\rho max}$ is 27.6 K at 8.7 GPa.

To clarify the behavior of the resistivity ρ around the magnetic ordering temperature T_N, we show the low-temperature resistivity in Fig. 8 (b), where the Néel temperature T_N is shown by an arrow. The pressure dependence of T_N is shown in Fig. 9. The Néel temperature T_N is almost pressure-independent up to 4.7 GPa. Above the pressure, T_N starts to increase with increasing pressure. T_N is 12.2 K at 8.7 GPa. A characteristic feature is that the sign of dT_N/dT changes at approximately 5 GPa. The present result is roughly consistent with that of the previous study up to 1.7 GPa.[18,19]

The resistivity below T_N is analyzed using the antiferromagnetic magnon model described as

$$\rho = \rho_0 + AT^2 + BT(1 + \frac{2T}{\Delta})\exp(-\frac{\Delta}{T}), \qquad (1)$$

where the third term corresponds to the contribution of the electron scattering by an antiferromagnetic magnon with an energy gap Δ, which was used in the analyses of URu_2Si_2 and $CePd_2Si_2$.[45,46] A fit of the resistivity data is shown by solid lines in Fig. 8 (b). The pressure dependences of the obtained parameters A and Δ are shown in Fig. 10 (a). A decreases simply with increasing pres-

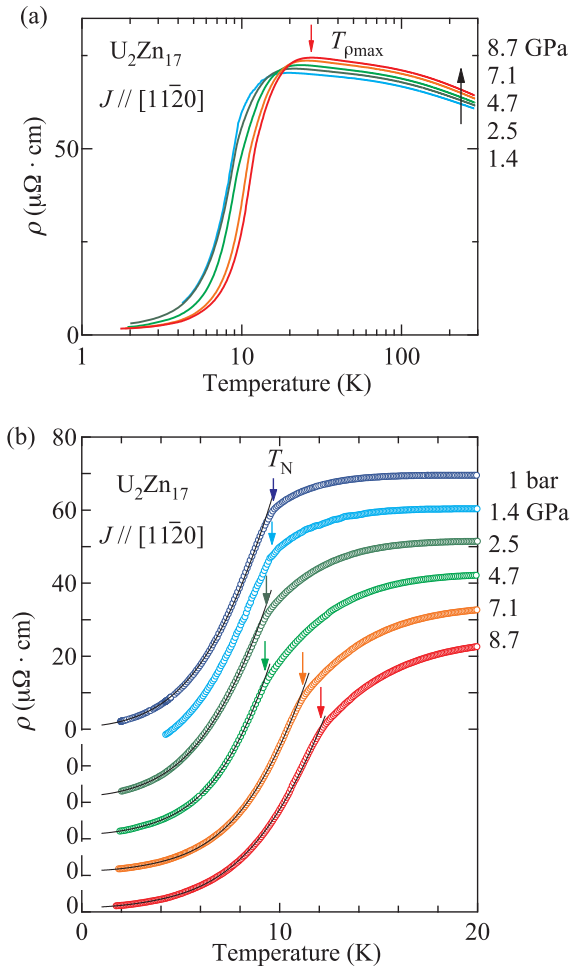

Fig. 8. (Color online) (a)Temperature dependences of the electrical resistivity ρ and (b) low-temperature resistivity at several pressures in U_2Zn_{17}.

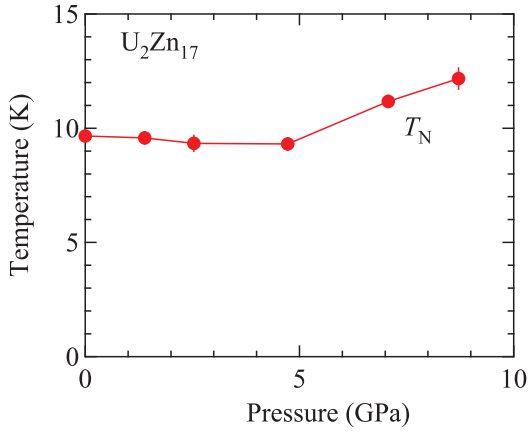

Fig. 9. (Color online) Pressure dependence of the Néel temperature T_N in U_2Zn_{17}.

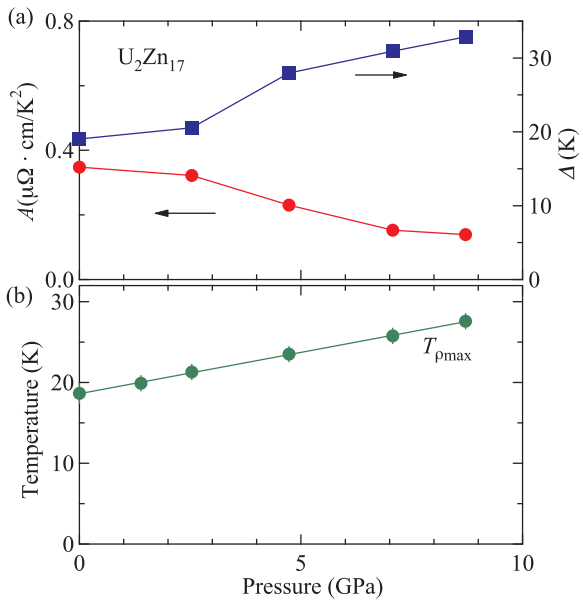

Fig. 10. (Color online) Pressure dependences of (a) the coefficient of T^2 term of the resistivity A(left side) and the antiferromagnetic gap Δ (right side), and (b) the characteristic temperature $T_{\rho max}$ where the resistivity ρ shows a maximum value in U_2Zn_{17}.

sure, from 0.35 $\mu\Omega$·cm/K^2 at 1 bar to 0.14 $\mu\Omega$·cm/K^2. The corresponding γ values are estimated as 190 and 120 mJ/K^2·mol at 1 bar and 8.7 GPa, respectively, using the Kadowaki-Woods relation ($A/\gamma^2 = 1.0\times10^{-5}$).[47] The estimated γ at 1 bar is consistent with the observed value of about $\simeq$ 200 mJ/K^2·molU. It is suggested that γ decreases with increasing pressure. Δ increases monotonically from 19 K at 1 bar to 33 K at 8.7 GPa, indicating that the antiferromagnetic state is enhanced with increasing pressure.

Very recently, Sidorov, *et al.* performed the resistivity and ac heat capacity measurements on U_2Zn_{17} up to 5.5 GPa.[48] The reported pressure dependence of T_N is roughly consistent with that observed in the present study. In the study, two successive magnetic transitions were observed in the pressure range of 2.64 - 3.25 GPa. It was concluded that the antiferromagnetic ground state changes to a new antiferromagnetic phase at approximately 2.4 GPa. Since we have not investigated the pressure dependence of T_N in detail at approximately this pressure, the change of the magnetic ground state is not discussed within the present data. We only mention the possibility that the slight change in the pressure dependences of A and Δ at approximately 3 GPa shown in Fig. 10 (a) is due to the appearance of the pressure-induced new magnetic phase revealed by our work.

Figure 10 (b) shows the pressure dependence of $T_{\rho max}$. This characteristic temperature $T_{\rho max}$ varies linearly as a function of pressure, shown as a solid straight line in the Fig. 10 (b). The pressure derivative of $\partial T_{\rho max}/\partial P$ is 1.0 K/GPa. Noted that $T_{\rho max}$ corresponds to the characteristic temperature T_0 of the electronic state in U_2Zn_{17}. The Grüneisen parameter Γ_{T_0} for T_0 is written as fol-

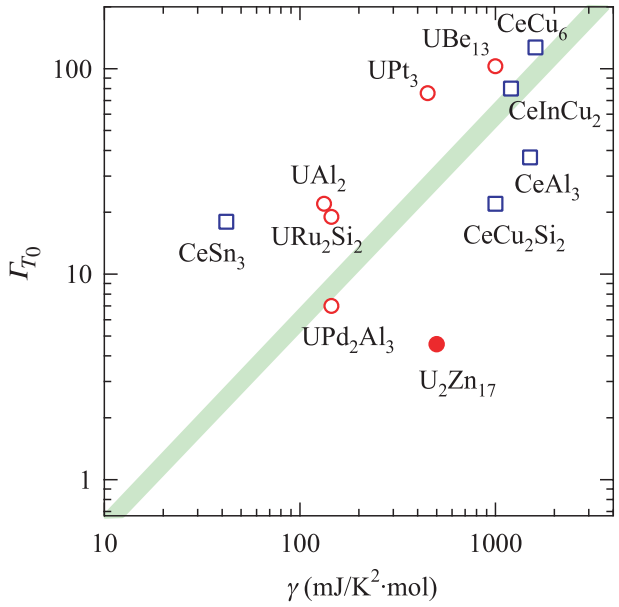

Fig. 11. (Color online) Grüneisen parameter Γ_{T_0} vs linear heat capacity coefficient γ for several cerium and uranium compounds.[19,50,51] The bold line is a guide to the eye.

lows:

$$\Gamma_{T_0} = -\frac{\partial \ln T_0}{\partial \ln V} = B\frac{1}{T_0}\frac{\partial T_0}{\partial P}, \qquad (2)$$

where B is the bulk modulus, estimated to be 83 GPa at 297 K for U_2Zn_{17} by ultrasound measurement.[49] The Grüneisen parameter Γ_{T_0} is 4.6 in U_2Zn_{17}. This value is small compared with those of heavy-fermion compounds, where the Grüneisen parameter is usually about one or two orders of magnitude larger than those of ordinary metals.[19,50,51] For example, the Grüneisen parameters for the characteristic temperature T_0 of the heavy-fermion superconductors $CeCu_2Si_2$, UBe_{13}, UPt_3, and URu_2Si_2 are 22, 103, 76, and 19, respectively.[19,50] In Fig. 11, we plot the relations of the Grüneisen parameter Γ_{T_0} and the electronic specific heat coefficient γ for several cerium and uranium heavy-fermion compounds.[19,50–52] Theoretically, the γ value correlates with the Grüneisen parameter enhanced by the many-body effect in the Kondo lattice system.[53,54] It is supposed that the Grüneisen parameter of U_2Zn_{17} is unusually small when the large γ value is taken into account. The Grüneisen parameter Γ_A for A in the resistivity is estimated as 2.5 in the low-pressure region. This value is also small compared with those of UBe_{13} and UPt_3, where the values of Γ_A are 17 and 61, respectively.[19] These small values of the Grüneisen parameters suggest that the electronic state in U_2Zn_{17} is not so sensitive to the change of the lattice parameters compared with those of the other heavy-fermion compounds with the order of $\gamma = 100$ mJ/K^2·mol.

It is interesting to note that the antiferromagnetic state in U_2Zn_{17} is very sensitive to a small amount of substitution on the Zn site.[55] The antiferromagnetic transition temperature T_N is strongly depressed to below 1.5 K with the substitution of only 2% Cu on the Zn site. On the other hand, the magnetic ordered state does not seem to be easily destroyed by high pressure. A much higher pressure far above 10 GPa seems to be needed to suppress the magnetic ordered state.

We compare the pressure effect on the antiferromagnetic state in U_2Zn_{17} with the cerium antiferromagnetic compounds $CeIn_3$ and $CeRhIn_5$ whose bulk moduli of 67 and 78, respectively, are close to that of U_2Zn_{17}.[56,57] Both $CeIn_3$ and $CeRhIn_5$ order antiferromagnetically at T_N =10 K and 3.8 K, respectively, at ambient pressure. Under high pressure, the antiferromagnetic ordering temperature T_N becomes 0 K at critical pressures P_c of 2.1 and 2.5 GPa, respectively, and the ground state changes into the superconducting one at approximately P_c. The magnetic to non-magnetic transition takes place below 3 GPa in both compounds whose compressibility β (= $1/B$) is similar to that of U_2Zn_{17}. On the other hand, the antiferromagnetic ordered state in U_2Zn_{17} is not easily destroyed, but is stabilized under high pressures of up to 9 GPa. The pressure effect on the antiferromagnetic phase as well as on the paramagnetic electronic state in U_2Zn_{17} is thus highly different from those of the heavy-fermion cerium compounds described basically by the Doniach model for the Kondo lattice. The weak pressure effect on T_N may be ascribed to the itinerant character of the $5f$ electrons in U_2Zn_{17}, as discussed in uranium monochalcogenides UX(X=Te, Se, S).[58–61] The pressure dependence of the Curie temperature T_C in uranium monochalcogenides deviates from that in the Doniach model, but is explained by the spin fluctuation theory of an itinerant $5f$ electron system based on the Hubbard model.[62,63] In the theory, the pressure-induced increase in the hydridization between $5f$ and conduction electrons strengthens the exchange interaction J between uranium ions, but it also decreases the $5f$ spectral weight (magnetic moment) at the uranium site. The model predicts a much more gradual demagnetization of the itinerant magnetic system under higher pressure than the Doniach picture. The present weak pressure dependence of T_N in U_2Zn_{17} may reflect the itinerant character of the $5f$ electrons in the compound, which is different from the $4f$ electron system in cerium compounds. It is interesting to note high-pressure studies of the well-known heavy-fermion antiferromagnet UCu_5 where the antiferromagnetic phase transition takes place at $T_N = 15.9$ K. It was revealed that the Néel temperature T_N of UCu_5 increases with increasing pressure very gradually at a rate of 0.33 K/GPa and that the magnetic phase exists even at 13 GPa.[64,65] It is suggested that the pressure response of uranium heavy fermion compounds with the antiferromagnetic ground state generally differs from that of the $4f$ electron system in cerium compounds.

4. Conclusions

We have performed a high-field magnetization experiment as well as a high-pressure experiment on single crystals of U_2Zn_{17} grown by the Bridgman method. We also measured the electrical resistivity and magnetic susceptibility at ambient pressure. The experimental results are summarized as follows:

1) Both the magnetic susceptibility χ and electrical resistivity ρ at ambient pressure show a broad maximum at approximately 18 K in the paramagnetic state above T_N, similarly to those observed in the heavy-fermion superconductors UPt_3, UPd_2Al_3, and URu_2Si_2, which is consistent with the results of the previous studies. The magnetic susceptibility is anisotropic between $H \parallel [0001]$ and $H \perp [0001]$, but the anisotropy of the susceptibility is not present betweeen $H \parallel [11\bar{2}0]$ and $H \parallel [10\bar{1}0]$. The resistivity ρ for $J \parallel [11\bar{2}0]$ is approximately half as small as that for $J \parallel [0001]$ above T_N.
2) In the antiferromagnetic state below T_N, the metamagnetic transition is observed at $H_c = 30$ T in the field along the antiferromagnetic easy axis of $[11\bar{2}0]$. The magnetic phase diagram for the field along the $[11\bar{2}0]$ direction is given. The magnetization shows the metamagnetic behavior at $H_m \simeq 35$ T in the paramagnetic state above T_N. We suggest that the behavior of the magnetization is the same as those observed in heavy-fermion compounds such as UPt_3, UPd_2Al_3, and URu_2Si_2.
3) From the high-pressure experiment using the diamond anvil cell, it was clarified that the antiferromagnetic ordering temperature T_N is almost pressure-independent up to 4.7 GPa and starts to increase in the higher-pressure region. The critical pressure for the magnetically ordered state seems to be far above 10 GPa.
4) The Grüneisen parameter Γ_{T_0} for the characteristic temperature T_0 was estimated to be 4.6 for U_2Zn_{17} from the pressure dependence of $T_{\rho max}$, where the resistivity ρ shows a maximum value. The value of the parameter is small compared with those of the other heavy fermion compounds, of which the electronic specific heat linear coefficient γ is in the order of 100 $mJ/K^2 \cdot mol$, indicating a small response of the electronic state to a change of the lattice parameter.

5. Acknowledgements

This work was financially supported by a Grant-in-Aid for Scientific Research on Innovative Areas "Heavy Electrons (No. 20102002), Scientific Research S (No. 20224015), C (No. 21540373, 22234567), Specially Promoted Research (No. 20001004) and Osaka University Global COE Program (G10) from the Ministry of Education, Culture, Sports, Science and Technology (MEXT) and Japan Society of the Promotion of Science (JSPS).

1) Y. Ōnuki and A. Hasegawa: *Handbook on the Physics and Chemistry of Rare earths*, ed. K. A. Gschneidner, Jr. and L. Eyring (Elsevier, Amsterdam, 1995) Vol. **20**, p. 1.
2) J. Flouquet: Prog. Low Temp. Phys. **15** (2006) 139.
3) H. v. Löhneysen, A. Rosch, M. Vojta, and P. Wölfle: Rev. Mod. Phys. **79** (2007) 1015.
4) S. Doniach: Physica **91B** (1977) 231.
5) D. Jaccard, K. Behnia, and J. Sierro: Phys. Lett. A **163** (1992) 475.
6) R. Movshovich, T. Graf, D. Mandrus, J. D. Thompson, J. L. Smith, and Z. Fisk: Phys. Rev. B **53** (1996) 8241.
7) N. D. Mathur, F. M. Grosche, S. R. Julian, I. R. Walker, D. M. Freye, R. K. W. Haselwimmer, and G. G. Lonzarich: Nature **394** (1998) 39.
8) H. Hegger, C. Petrovic, E. G. Moshopoulou, M. F. Hundley, J. L. Sarrao, Z. Fisk, and J. D. Thompson: Phys. Rev. Lett. **84** (2000) 4986.
9) S. S. Saxena, P. Agarwal, K. Ahllan, F. M. Grosche, R. K. W. Haselwimmer, M. J. Steiner, E. Pugh, I. R. Walker, S. R. Julian, P. Monthoux, G. G. Lonzarich, A. Huxley, I. Sheikin, D. Braithwaite, and J. Flouquet: Nature **406** (2000) 587.
10) A. Huxley, I. Sheikin, E. Ressouche, N. Kernavanois, D. Braithwaite, R. Calemczuk, and J. Flouquet: Phys. Rev. B **63** (2001) 144519.
11) T. Akazawa, H. Hidaka, H. Kotegawa, T. C. Kobayashi, T. Fujiwara, E. Yamamoto, Y. Haga, R. Settai, and Y. Ōnuki: J. Phys.: Condens. Matter **16** (2004) L. 29.
12) T. Akazawa, H. Hidaka, H. Kotegawa, T. C. Kobayashi, T. Fujiwara, E. Yamamoto, Y. Haga, R. Settai, and Y. Ōnuki: J. Phys. Soc. Jpn. **73** (2004) 3129.
13) H. R. Ott, H. Rudigier, P. Delsing, and Z. Fisk: Phys. Rev. Lett **52** (1984) 1551.
14) H. E. Fischer, E. T. Swartz, R. O. Pohl, B. A. Jones, J. W. Wilkins, and Z. Fisk: Phys. Rev. B **36** (1987) 5330.
15) D. E. Cox, G. Shirane, S. M. Shapiro, G. Aeppli, Z. Fisk, J. L. Smith, J. Kjems and H. R. Ott: Phys. Rev. B **33** (1986) 3614.
16) G. Aeppli and C. Broholm: *Handbook on the Physics and Chemistry of Rare Earths*, ed. K. A. Gschneider, Jr. and K. Eyring (Elsevier, North-Holland, 1994) Vol. **19** chap.123.
17) J. O. Willis, Z. Fisk, R. M. Aikin, M. W. McElfresh, J. D. Thompson, E. Zirngiebl, J. A. O'Rourke and J. L. Smith: J. Appl. Phys. **61** (1987) 4373.
18) J. D. Thompson, Z. Fisk, and H. R. Ott: J. Magn. Magn. Mat. **54-57** (1986) 393.
19) J. D. Thompson, and J. M. Lawrence: *Handbook on the Physics and Chemistry of Rare Earths*, ed. K. A. Gschneider, Jr. and K. Eyring (North-Holland, 1994) Vol. **19**, chap.133.
20) D. J. Dunstan and I. L. Spain: J. Phys. E: Sci. Instrum. **22** (1989) 913.
21) I. L. Spain and D. J. Dunstan: J. Phys. E: Sci. Instrum. **22** (1989) 923.
22) J. Thomasson, Y. Dumont, J.-C. Griveau, and C. Ayache: Rev. Sci. Instrum. **68** (1997) 1514.
23) G. Knebel, M-A. Méasson, B. Salce, D. Aoki, D. Braithwaite, J. P. Brison, and J. Flouquet: J. Phys.: Condens. Matter **16** (2004) 8905.
24) P. M. Bell and H. K. Mao: Carnegie Inst. Wash. Yearb. **80** (1981) 404.
25) Z. Liu, Q. Cui and G. Zou: Physics Letters A **143** (1990) 79.
26) N. Tateiwa and Y. Haga: Rev. Sci. Instrum. **80** (2009) 123901.
27) R. A. Forman, G. J. Piermarini, J. D. Barnett, and S. Block: Science **176** (1972) 284.
28) J. D. Barnett, S. Block, and G. J. Piermarini: Rev. Sci. Instrum. **44** (1973) 1.
29) G. J. Piermarini, S. Block, J. D. Barnett, and R. A. Forman: J. Appl. Phys. **46** (1975) 2774.
30) C.-S. Zha, H. K. Mao, and R. J. Hemley: Proc. Natl Acad. Sci. USA **97** (2000) 13494.
31) T. Siegrist and Y. Le Page: J. Less-Common Metal. **127** (1987) 189.
32) L. M. Gelato and E. Parthé: J. Appl. Cryst. **20** (1987) 139.
33) T. Siegrist, M. Olivier, S. P. McAlister, and R. W. Cochrane: Phys. Rev. B **33** (1986) 4370.
34) C. Broholm, J. K. Kjem, G. Aeppli, Z. Fisk, J. L. Smith, S. M. Shapiro, G. Shirane, and H. R. Ott: Phys. Rev. Lett. **58** (1987) 917.
35) K. Sugiyama, M. Nakamura. D. Aoki, K. Kindo, N. Kimura, H. Aoki, T. Komatsubara, S. Uji, Y. Haga, E. Yamamoto, and Y. Ōnuki: Phys. Rev. B **60** (1999) 9248.
36) K. Sugiyama, M. Nakashima, H. Ohkuni, K. Kindo, Y. Haga, T. Honnma, E. Yamamoto, and Y. Ōnuki: J. Phys. Soc. Jpn. **68** (1999) 3394.
37) K. Oda, K. Sugiyama, N. K. Sato, T. Komatsubara, K. Kindo, and Y. Ōnuki: J. Phys. Soc. Jpn. **68** (1999) 3115.
38) Y. Kuramoto and K. Miyake: J. Phys. Soc. Jpn. **59** (1990) 2831.
39) K. Miyake and Y. Kuramoto: Physica B **171** (1991) 20.
40) Y. Ōno: J. Phys. Soc. Jpn. **67** (1998) 2197.
41) K. Ohara, K. Hanazawa, and K. Yoshida: J. Phys. Soc. Jpn.

68 (1999) 521.
42) F. J. Ohkawa: Solid State Commun. **71** (1989) 907.
43) H. Satoh and F. J. Ohkawa: Phys. Rev. B **57** (1998) 5891.
44) H. Satoh and F. J. Ohkawa: Phys. Rev. B **63** (2001) 184401.
45) T. T. M. Palstra, A. A. Menovsky, and J. A. Mydosh: Phys. Rev. B **33** 6527 (1986) 6527.
46) S. Raymond and D. Jaccard: Phys. Rev. B **61** (2000) 8679.
47) K. Kadowaki and S. B. Woods: Solid State Commun. **58** (1986) 507.
48) V. A. Sidorov, J. D. Thompson, and Z. Fisk: J. Phys.: Condens. Matter **22** (2010) 406002.
49) A. Migliori, J. L. Sarrao, D. Mandrus, Z. Fisk, A. Balatsky, S. A. Trugman, J. D. Thompson, and M. B. Maple: Physica B **199**&**200** (1994) 36.
50) T. Kagayama, G. Oomi, K. Iki, N. Mori, Y. Ōnuki, and T. Komatsubara: J. of Alloys Compds. **213-214** (1994) 387.
51) T. Kagayama, G. Oomi, E. Ito, Y. Ōnuki, and T. Komatsubara: J. Phys. Soc. Jpn. **63**, 3927 (1994) 3927.
52) P. Link, D. Jaccard, C. Geibel, C. Wassilew, and F. Steglich: J. Phys.: Condens. Matter **7** (1995) 373.
53) T. M. Hong, Phys. Rev. B. **46** (1992) 13862.
54) J. Flouquet, A. Barla, R. Boursier, J. Derr, and G. Knebel: J. Phys. Soc. Jpn. **74** (2005) 178.
55) J. O. Willis, Z. Fisk, G. R. Stewart, and H. R. Ott: J. Magn. Magn. Mat. **54-57** (1986) 395.
56) I. Vedel, A. M. Redon, J. -M. Mignot, J. M. Leger: J. Phys. F: Met. Phys. **17** (1987) 849.
57) R. S. Kumar, A. L. Cornelius, and J. L. Sarrao: Phys. Rev. B **70** (2004) 214526.
58) P. Link, U. Benedict, J. Wittig, and H.Wühl: J. Phys.: Condens. Matter **4** (1992) 5585.
59) P. Link, U. Benedict, J. Wittig, and H.Wühl: Physica B **190** (1993) 68.
60) C. Y. Huang, F. J. Laskowski, C. E. Olsen, and J. L. Smith: J. Phys. **40** C4 (1979) 26.
61) A. L. Cornelius, J. S. Schilling, O. Vogt, K. Mattenberger, and U. Benedict: J. Magn. Magn. Mat. **161** (1996) 169.
62) B. R. Cooper, Q. G. Sheng, U. Benedict, and P. Link: J. Alloys. Comp. **213-214** (1994) 120.
63) Q. G. Sheng and B. R. Cooper: J. Magn. Magn. Mat. **164** (1996) 335.
64) J. D. Thompson: J. Magn. Magn. Mat. **63-64** (1987) 358.
65) M. Nakashima, I. Sugitani, Y. Okuda, H. Shishido, T. D. Matsuda, Y. Haga, M. Hedo, Y. Uwatoko, R. Settai, and Y. Ōnuki: *Frontiers of Basic Science towards New Physics Earth and Space Science Mathematics*, eds. H. Takabe, N. H. Luong, and Y. Ōnuki (Osaka University Press, Osaka, 2006) 267.